https://doi.org/10.1038/s44384-025-00013-w

Theoretical developments and experimental Insights of acoustic and elastic bound states in the continuum

Liangshu He[1,2], Shengming Sun[2], Ricardo Martin Abraham-Ekeroth[2,3,4,5], Yabin Jin[6,7] ✉, Yanxun Xiang[6] & Dani Torrent[2] ✉

This paper explores recent theoretical advancements and experimental observations of bound states in the continuum (BICs) in acoustic, elastic, and optomechanical systems. We focus on three main types of BICs: symmetry-protected, Friedrich-Wintgen, and Fabry-Pérot BICs, and discuss their extensions to complex systems. Our work aims to bridge the theoretical and experimental validations of BICs, highlighting their utility and future development in mechanical wave systems.

High-quality wave localization has long been a topic of intense exploration. Recently, bound states in the continuum have garnered considerable attention due to their infinite quality factors in open resonant systems. Specifically, BICs describe a class of localized states that exists in the continuum radiation spectrum of a spatially confined open system. This is counterintuitive, because an open resonant system will inevitably couple with the external radiation state and lead to energy leakage, thus energy losses are usually unavoidable. However, due to some special conditions such as symmetry mismatch or destructive interference, certain modes are separated from the radiated waves and thus become eigenmodes with real frequencies. The resonant energy of these modes is fully localized, and their lifetimes extend to infinity, defining them as bound states in the continuum or trapped modes. BICs were first mathematically proven by von Neumann and Wigner in the field of quantum mechanics in 1929[1], and subsequently expanded by Stillinger and Herrick in atomic and molecular systems[2]. Although the concept originated from quantum mechanics, the development of wave physics, such as electromagnetic, acoustic and elastic waves has provided simple platforms for effectively observing BICs in experiments.

It is worth mentioning that although BICs have infinite radiation quality factors in theory, they are ideal situations from pure mathematics. Due to many factors such as manufacturing errors, limited sample size, and material viscous effects, the quality factor of BICs can only be finite, which is regarded as quasi-BICs. For BICs based on symmetry mismatch, since the manufacturing structure usually does not have strict symmetry rules, the localized modes cannot be completely decoupled from the radiation continuum, resulting in leakage. For the BICs based on destructive interference, energy will leak unless the geometric parameters and frequency satisfy the destructive interference conditions. Nevertheless, one can achieve quasi-BICs to realize compact wave functional devices such as sensors, filters, and low-threshold lasers with high quality factors. Some excellent review articles summarize the recent efforts in the field of BICs from different perspectives, including formation mechanisms of BICs[3,4], BICs in resonant nanostructures[5], applications of photonic BICs[6,7], and acoustic resonances[8].

In this perspective paper, we start from the introduction of types and formation mechanisms of BICs, then provide a comprehensive evaluation of the current research trends on BICs by analyzing key developments across a wide range of disciplines, including acoustics, elasticity, topology and optomechanics. This cross-disciplinary perspective enables a deeper understanding of BICs and uncovers novel opportunities for innovation and practical applications that might be overlooked when confined to a single research domain. By presenting this holistic view, the current work serves as a valuable resource for researchers looking to explore the untapped potential of BICs in emerging technologies.

Types and formation mechanisms of BICs

For the two-dimensional phononic crystals composed of periodic holes as shown in Fig. 1a, its wave vector $\boldsymbol{k}$ can be decomposed into out-of-plane ($\boldsymbol{k}_\perp$) and in-plane ($\boldsymbol{k}_\parallel$) components which are related by

$$\boldsymbol{k}_\perp = \sqrt{\omega^2/c^2 - \boldsymbol{k}_\parallel{}^2} \tag{1}$$

where c is the bulk wave velocity. The corresponding momentum space is divided into two regions by $\omega = c\boldsymbol{k}_\parallel$ (sound line), as shown in Fig. 1b. Below

[1]School of Aerospace Engineering and Applied Mechanics, Tongji University, 200092 Shanghai, China. [2]GROC, UJI, Institut de Noves Tecnologies de la Imatge (INIT), Universitat Jaume I, 12071 Castelló de la Plana, Spain. [3]Instituto de Física Arroyo Seco (IFAS), Pinto 399, 7000 Tandil, Argentina. [4]Centro de Investigaciones en Física e Ingeniería del Centro de la Provincia de Buenos Aires (UNCPBA-CICPBA-CONICET), Campus Universitario UNCPBA, 7000 Tandil, Argentina. [5]Consejo Nacional de Investigaciones Científicas y Técnicas (CONICET), Godoy Cruz 2290 (C1425FQB), Buenos Aires, Argentina. [6]Shanghai Key Laboratory of Intelligent Sensing and Detection Technology, School of Mechanical and Power Engineering, East China University of Science and Technology, 200237 Shanghai, China. [7]Shanghai Institute of Aircraft Mechanics and Control, 200092 Shanghai, China. ✉e-mail: yabin.jin@ecust.edu.cn; dtorrent@uji.es

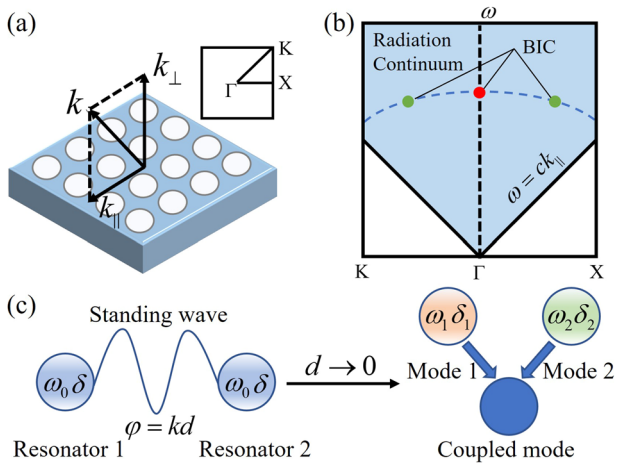

Fig. 1 | The concept and formation mechanism of different types of BICs. a Two-dimensional phononic crystals and Brillouin zone. $\boldsymbol{k}$ denotes wave vector with the out-of-plane ($\boldsymbol{k}_\perp$) and in-plane ($\boldsymbol{k}_\parallel$) components. **b** Symmetry-protected BICs (red dot) and accidental BICs (green dots) in the momentum space. The blue shaded area above the sound line ($\omega = c\boldsymbol{k}_\parallel$) represents the radiation continuum. **c** Left panel: Fabry-Pérot BICs. ω_0 and δ represent the resonance frequency and loss coefficient, respectively. φ is the phase shift, while d is the distance of the two resonators. Right panel: Friedrich-Wintgen BICs. ω and δ with different subscripts represent the resonance frequencies and loss coefficients of the two modes, respectively.

the sound line, $\boldsymbol{k}_\perp$ is a pure imaginary number, which means the related wave is evanescent, forming the regular bound states. On the contrary, radiating waves with real wave vectors $\boldsymbol{k}_\perp$ will occupy the entire blue region above the sound line, which is called the radiation continuum. Therefore, the traditional view is that all resonant modes in the radiation continuum have energy leakage. However, symmetry mismatch and destructive interference mechanisms provide opportunities for the emergence of BICs.

Based on the formation mechanisms, BICs can be roughly divided into three categories, including symmetry-protected (SP) BICs[9–12], Fabry-Pérot (FP) BICs[13,14], and Friedrich-Wintgen (FW) BICs[15–19]. SP BICs, as the simplest type, appear at Γ point and are formed by symmetry protection, see the red dot in Fig. 1b. Energy leakage is inhibited due to the spatial symmetry constraints of the system, which prevent specific modes from coupling with radiation states that possess different symmetry characteristics. This mechanism strictly depends on the symmetry of the structure. Any perturbation that preserves the symmetry will not affect the existence of SP BICs, granting them a certain degree of robustness. In the ΓX or ΓK region that deviates from Γ point (also called off-Γ points), at least one of the components of the in-plane wave vector $\boldsymbol{k}_\parallel$ ($\boldsymbol{k}_x$ and $\boldsymbol{k}_y$) will not be zero, and the strict symmetry will be destroyed, resulting in leakage. Relevant experimental works have shown that special BICs can exist in these regions, called accidental BICs as denoted by the green dots in Fig. 1b, and the basic mechanism has been given based on the polarization in the optical context[20,21]. Compared to electromagnetic and acoustic waves, the mechanism of accidental BICs in elastic waves, where longitudinal and transverse polarizations coexist, requires further exploration. The original definition of accidental BIC applies to the first Brillouin zone of infinite-periodic systems, where the radiation channel is accidentally closed by fine-tuning the physical parameters. Later, this concept was also extended to finite systems, where the Brillouin zone cannot be defined[8].

FP BICs arise from destructive interference between the resonances typically supported by two resonators. As shown in the left panel of Fig. 1c, the Fabry-Pérot cavity is formed by two identical resonators acting as a pair of mirrors. When the distance is adjusted so that the phase shift of round-trip wave is an integer multiple of 2π, a standing wave field forms inside the cavity, while destructive interference in the radiation channels traps the waves within the cavity. The fundamental mathematical interpretation of FP BICs can be derived from coupled-mode theory. The dynamic equations for a system of two resonators separated by a distance d are given as follows:

$$\frac{\mathrm{d}r_1}{dt} = i\omega_0 r_1 + \delta r_1 + i\kappa r_2 + \delta e^{i\varphi} r_2 \tag{2}$$

$$\frac{\mathrm{d}r_2}{dt} = i\omega_0 r_2 + \delta r_2 + i\kappa r_1 + \delta e^{i\varphi} r_1 \tag{3}$$

where ω_0 is the resonance frequency, δ the loss coefficient, κ the coupling strength between the resonators, $\varphi = kd$ is the phase shift, and the influence on each other caused by loss is described by $\delta e^{i\varphi}$. One step further, we have the matrix form

$$-i\partial_t|\psi\rangle = H|\psi\rangle \tag{4}$$

where $|\psi\rangle = (r_1, r_2)^T$ and the Hamiltonian is

$$H = \begin{bmatrix} \omega_0 - i\delta & \kappa - i\delta e^{i\varphi} \\ \kappa - i\delta e^{i\varphi} & \omega_0 - i\delta \end{bmatrix} \tag{5}$$

The eigenvalues are

$$\omega_\pm = \omega_0 \pm \kappa - i\delta\,(1 \pm e^{i\varphi}) \tag{6}$$

If we consider the phase shift of round-trip wave is 2π ($\varphi = \pi$), one of the eigenvalues simplifies to a real frequency $\omega_+ = \omega_0 + \kappa$, which is a FP BIC.

FW BICs are another kind of BICs based on destructive interference. When we consider the distance of the two resonators zero ($d = 0$), a real solution can be also theoretically obtained from Eq. (6). Actually, Friedrich and Wintgen[17] realized that for a single resonator, if we consider two modes with different resonance frequencies and loss coefficients, the coupling between the modes also provides an opportunity to form a BIC, as shown in the right panel of Fig. 1c. In this case, we can also apply the coupled-mode theory, but the Hamiltonian would be

$$H = \begin{bmatrix} \omega_1 - i\delta_1 & \kappa - i\sqrt{\delta_1\delta_2} \\ \kappa - i\sqrt{\delta_1\delta_2} & \omega_2 - i\delta_2 \end{bmatrix} \tag{7}$$

Thus, the eigenvalues are

$$\begin{aligned}\omega_\pm = &\frac{1}{2}(\omega_1 + \omega_2) - \frac{1}{2}i(\delta_1 + \delta_2) \\ &\pm \frac{1}{2}\sqrt{[\omega_1 - \omega_2 - i(\delta_1 - \delta_2)]^2 + 4(\kappa - i\sqrt{\delta_1\delta_2})^2}\end{aligned} \tag{8}$$

The condition for the existence of real solution is[22]

$$\kappa(\delta_1 - \delta_2) = \sqrt{\delta_1\delta_2}\,(\omega_1 - \omega_2) \tag{9}$$

Substituting Eq. (9) into Eq. (8), we get a FW BIC with real frequency

$$\omega_- = \frac{1}{2}(\omega_1 + \omega_2) - \frac{1}{2}\kappa\left(\sqrt{\frac{\delta_1}{\delta_2}} + \sqrt{\frac{\delta_2}{\delta_1}}\right) \tag{10}$$

We know that specific symmetry mismatch or destructive interference of resonances/modes is responsible for the formation of BICs. Additionally, the design of BICs in classical wave systems involves the complexity of polarization states. Therefore, research in BICs in acoustic, elastic, topological, and optomechanical systems has different challenges and application values, resulting in different levels of development at present.

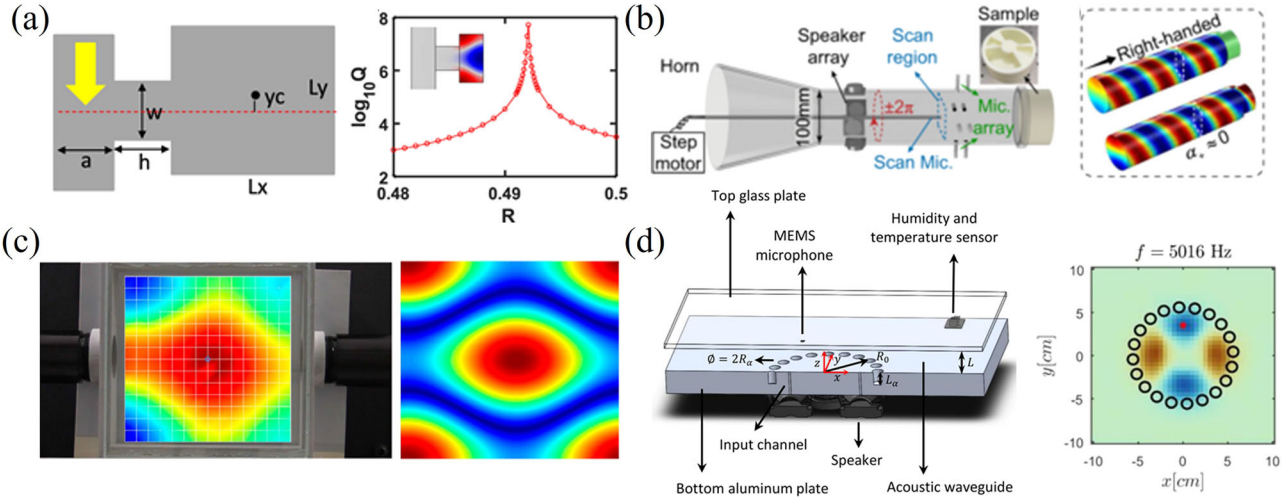

Fig. 2 | BICs in acoustic systems. a Acoustic resonator that can realize three types of BICs (SP, FW, and accidental BICs). The inset on the right shows the mirror-induced BIC. **b** Perfect EPs induced by chiral radiation quasi-BICs. The left panel is the experimental platform with sample and the right panel shows the complete reflection with right-handed incident wave. **c** Visualization of FW QBICs using laser Doppler vibrometer. The left panel shows the visualized sound pressure field of the QBIC within the experimental set-up, while the right shows the QBIC supported by dominant modes. **d** Measurement of BICs supported by circularly-arranged blind holes in two-dimensional, fully open space. The left panel is the experimental setup and the right is one BIC's modal shape. **a** is adapted from ref. 31. with permission, CC BY 4.0; **b** is adapted from ref. 37 with permission, Copyright 2023 American Physical Society; **c** is adapted from ref. 39 with permission, CC BY 4.0; **d** is adapted from ref. 40 with permission, CC BY 4.0.

Acoustic BICs

The development of acoustics plays a leading role in the expansion of BICs' research into the field of mechanical waves. As early as the end of the last century, a series of pioneering works by Evans et al. obtained numerical evidence of acoustic BICs in airborne acoustic waveguides and hydroacoustic systems[23–25]. In 2006, Sugimoto and Imahori further demonstrated that the acoustic waveguide connected to the Helmholtz resonator can trap sound waves[26]. Later, an important work by Hein et al. revisited the classical system of pipes with side-branched rectangular cavities in 2012[14]. The three types of trapped modes in the pipe cavity system, i.e., SP BICs, FW BICs and FP BICs, are fully confirmed and analyzed from a numerical perspective. They also discussed the phenomenon of transition to quasi-trapped modes due to energy leakage, which manifests as a Fano resonance with symmetric-antisymmetric characteristics. Lyapina et al. [27] obtained FW BICs by adjusting the length of the cavity in acoustic axisymmetric duct-cavity structures to meet full destructive interference condition. In their subsequent work[28], they added two waveguides on both sides of the resonator to form an asymmetric structure. This structure brings a freedom of azimuthal angle of the two waveguides, and explores the SP BIC obtained by adjusting this degree of freedom. In another interesting work presented by Sadreev et al. [29] square and triangular resonators with C_{4v} and C_{3v} symmetries were used to realize twofold-degenerated FW BICs, maintaining high quality factors over a range of larger size deviations compared to those for regular BICs. Such remarkable robustness helps overcome accuracy issues during the manufacturing procedure.

Later, experimental observations of acoustic BICs were successfully performed and showed the potential applications in acoustic sensors, filters, and harvesters. Farzad et al. [30] first included the topological Fano resonance into the category of BICs in 2019. From the perspective of simulation and experiment, this work revealed the basic principle of the dark mode existing as a local state in the bright mode continuum to form a SP BIC. In 2020, Huang et al. observed FW quasi-BICs from the designed detuned resonant cavity and discussed the possibility of arbitrarily increasing the quality factor of the BICs by increasing the opening width of the cavity and reducing the thermo-viscous losses[16]. In 2021, they found that by simple parameter adjustments, three types of BICs could be realized in a classical system consisting of a thin neck connecting a circular duct and a rectangular resonant cavity, as shown in Fig. 2a[31]. The SP BICs are determined by the position of the rectangular resonant cavity on the circular duct, and a slight offset form quasi-BICs, while the FW BICs depend on the size ratio of the cavity to induce mode interference. More importantly, this work proposed the new concept of mirror-induced BICs. The principle is that if the eigenmodes (BICs) of a full-sized cavity (see the left panel of Fig. 2a) are symmetric, BICs can also be found by constructing a semi-structure (right panel of Fig. 2a). The direction in which the structure is halved can be chosen according to the symmetry of the eigenmodes. In 2022, Huang et al. studied the super-cavity resonance in a system of two coupled cavities[32]. By adjusting the distance between the cavities, they observed moving, merging, and vanishing of FW BICs. Subsequently, they reported another work based on parameter adjustment of BICs in a coupled acoustic waveguide-resonant system[18]. In general, there are two main contributions. First, both single-port and two-port structures can support FW BICs. Second, when the ports are adjusted to some specific positions, BICs can still be supported despite the structural asymmetry. These BICs are analogous to the accidental BICs found at off-Γ points in momentum space, see Section II and Fig. 1b. Moreover, a recent theoretical work by Yin et al. [33] showed that by introducing rotational obstacles, some accidental BICs can be obtained at specific rotation angles. The method of realizing accidental BICs is similar to that in ref. 18 in a sense that, by continuously adjusting the port positions, one can switch from FW to SP BICs or accidental BICs. Based on this work, they further explored the asymmetric structure consisting of two waveguides connected to a rectangular or cylindrical resonator, and discovered a series of SP and accidental BICs[12]. To enrich the freedom of the BICs-modulation, they introduced the concept of "bridging near-field coupling" to adjust the FW BICs of two asymmetric acoustic cavities[19], showing that the near-field coupling can be changed by adjusting the diameter and position of the bridge tube to achieve FW or quasi-BICs. When the adjustment is appropriate, the radiation loss completely compensates for the intrinsic loss of the system, and perfect absorption can be consequently achieved. In non-Hermitian physics that considers dissipation in the system, exceptional points (EPs) are a special type of frequency points that support asymmetric scattering[34,35]. In a recent work, perfect EPs induced by chiral radiation quasi-BICs were demonstrated[22,36], whose characteristic is weak chiral radiation, as shown in Fig. 2b[37]. The left panel shows the experimental

platform and chiral meta-surface sample. The incident sound vortex is generated by setting the phase of the speaker array, the right panel shows the complete wave reflection from the sample with right-handed incident wave at perfect EP. On the contrary, the incident wave will be absorbed completely with left-handed polarization, so that the system exhibits extreme asymmetry.

Krasikova et al. [38] presented an experimental study by using a pair of coupled C-shaped Helmholtz resonators. Quasi-BICs and EPs can be achieved by adjusting the relative distance or intrinsic loss. An experimental work done by Kronowetter et al. in 2023 brought research on acoustic BICs into a new perspective[39]. They designed a sample with high-transmission glass side walls, which can support FW BICs, using laser Doppler vibrometer to measure the transmission spectrum and plotting the sound pressure field inside the cavity, as shown in Fig. 2c. Direct visualization provides essential information about the formation of BICs, such as field strength distribution and loss inside the cavity. Based on this visualization, the authors further demonstrated the optimized reconstruction of QBIC. The dominant modes were screened out after performing the fast Fourier transform on the original sound field, and the QBIC supported by these modes was reconstructed by inverse fast Fourier transform, as shown in the right panel of Fig. 2c. In a recent work, Martí-Sabaté et al. [40] used a Micro-Electro-Mechanical System (MEMS) based microphone to conduct a comprehensive visual characterization of the BICs formed by a structure with circularly-arranged blind holes, as shown in Fig. 2d. Unlike zero- or one-dimensional BICs that are confined in a cavity, their BICs were formed by confining energy to two-dimensional, fully open space through clusters of scatterers, whose structure has a large number of open boundaries.

In general, the acoustic systems serve as excellent experimental platforms, enabling rapid development of acoustic BICs and their practical applications. The future of acoustic BICs may focus on the development of advanced acoustic devices that require ultrahigh Q-factors, such as acoustic emission-enhancement devices, which have been demonstrated by acoustic emission experiments based on BICs[41]; highly sensitive sensors based on the extreme acoustic confinement caused by BICs[16,31] and perfect sound absorbers based on extremely asymmetric chiral BICs[37]. Strong localization properties can also make acoustic devices more compact, which will help the development of miniature devices such as micro sensors and other ultrasonic transmission equipment.

Elastic BICs

In the practical development of quantum to classical waves, BICs have been fully verified in electromagnetic, water, and airborne acoustic waves. However, the research progress of BICs on elastic waves in solid systems is relatively slow since there are more wave modes involved in elastic media[42,43]. This turns more difficult to conduct theoretical analysis and experimental observation. Recently, several excellent works on elastic BICs have been shown in the literature. Clamping losses exist in the connections between different elements of mechanical systems and result in mechanical energy dissipation. Chen et al. [44] found that the elastic energy dissipation in resonant, stem-supported microsphere or micro-disk structures, can be reduced by the concept of SP BICs. They succeeded in confining the mechanical waves in the microsphere or micro-disk based on the modes decoupling from the stem. This was done by designing suitable clamp conditions to induce symmetry mismatch. Later, Zhao et al. [45] further revealed the SP BICs of slab-on-substrate optomechanical crystals through numerical simulations. Group theory methods were applied to identify all the mechanical BICs at Γ point in momentum space and explored the coupling between mechanical BICs and optical modes. Traditional optomechanical structures adopt a suspended configuration to avoid energy leakage to the substrate, which leads to problems such as slow heat dissipation. A BICs-based mechanism was used to change the configuration, which helped to solve the problem fundamentally. Another experimental work concerning the mechanical BICs in optomechanical micro-resonators to reduce the clamping loss was done by Yu et al. [46]. They studied a kind of wheel-shaped thin-plate resonator in which the so-called radial-contour mode and wine-glass mode coupling caused destructive interference. The principle is that the two dissipative modes of a single resonator couple with each other to form a FW BIC. The energy was trapped in the wheel-shaped structure with low leakage to the supporting structure. Generally, energy dissipation caused by clamping loss is one of the main challenges in the manufacturing of optomechanical systems, and greatly limits their application to precision metrology equipment. Traditional approaches to reduce the clamping loss include surrounding the resonator with phononic band-gap structures[47], minimizing the supporting structures[48], supporting the resonator at its nodal points[49], and so forth. Studies on BICs in optomechanical micro-resonators have, to a certain extent, opened new possibilities for building high-quality nanomechanical resonators. The mechanism of BICs can enhance manufacturing processes while maintaining high-quality factors.

In 2021, Cao et al. [50] designed a perfect absorber for bending waves in elastic beams based on the FW quasi-BICs principle. With the support of BICs, this absorber no longer relies on traditional damping materials, thus potentially circumventing problems such as poor heat resistance. At the same time, they reported the use of quasi-BICs to achieve perfect mode conversion between flexural and longitudinal waves, as shown in Fig. 3a. The possibility of transforming quasi-BICs into BICs by utilizing the FP resonance frequency was discussed[51]. Haq et al. [52] demonstrated theoretical work on realizing FP BICs based on two cylindrical scattering arrays embedded in a matrix medium. The most important result is that, by adjusting the distance between the arrays, destructive interference of in-plane transverse and longitudinal modes can be achieved at some specific values of the Bloch phase, or ratio of the phase velocities, thereby obtaining an analytical solution of BICs. In 2022, Deriy et al. [53] stated that if a solid resonator with rotational symmetry is placed in gas or non-viscous fluid, its torsional mode is a genuine BIC in finite structure. This is because the torsional modes will be completely separated from the environment that supports only longitudinal waves. Rahman et al. [54] indicated FP BICs in some compact regions induced by adding defects to the spring-mass chains or waveguide arrays. As a natural extension of spring-mass chains, they have extended the same concept to structural beams in their recent work[55]. They made FP BICs by adding side beams in arbitrarily compact regions. Jin et al. [56] also reported the formation of FP BICs in a thin plate with two lines of pillars deposited on top. Martí-Sabaté et al. [57] developed the quasi-BICs of elastic flexural waves in symmetric clusters of scatterers when placed regularly around the circumference of the circle. They found that the quality factor is proportional to the number of scatterers and will theoretically go to infinity if the scatterers form a cylinder. In addition, they also revealed the phenomenon that energy in high multipolar orders gathers at the border to form whispering gallery modes, as shown in Fig. 3b. In another work, Lee et al. [58] embedded the acoustic cavity into the elastic beam and realized FP quasi-BIC through acoustic-elastic interaction in experiments. Their work revealed that under the action of acoustic-elastic coupling, in-plane elastic waves can be effectively trapped. Gao et al. [59] introduced silica as an inclusion to a silicon plate. In this way, they realized the quasi-BICs of Lamb waves by utilizing the total internal reflection mechanism caused by the wave velocity of the inclusion being lower than that of the matrix. An et al. [60] designed a Lamb waveguide with two pairs of side-branch resonant pillars, as shown in Fig. 3c. Their work fully reveals (from theory and experiment) that the monopolar or dipolar oscillations of pillar resonators under symmetric configurations will lead to symmetric and antisymmetric quasi-BICs.

Overall, the development of elastic BICs is relatively lagging due to experimental difficulties. With more experimental input, research on elastic BICs is moving towards the design of highly efficient devices, such as ultra-narrowband filters, high-Q resonators, and highly sensitive sensors. In addition, the development of tunable BIC structures is also one of the main directions, which can respond to external fields or dynamically adapt, such as achieving efficient energy conversion or storage through highly localized wave properties.

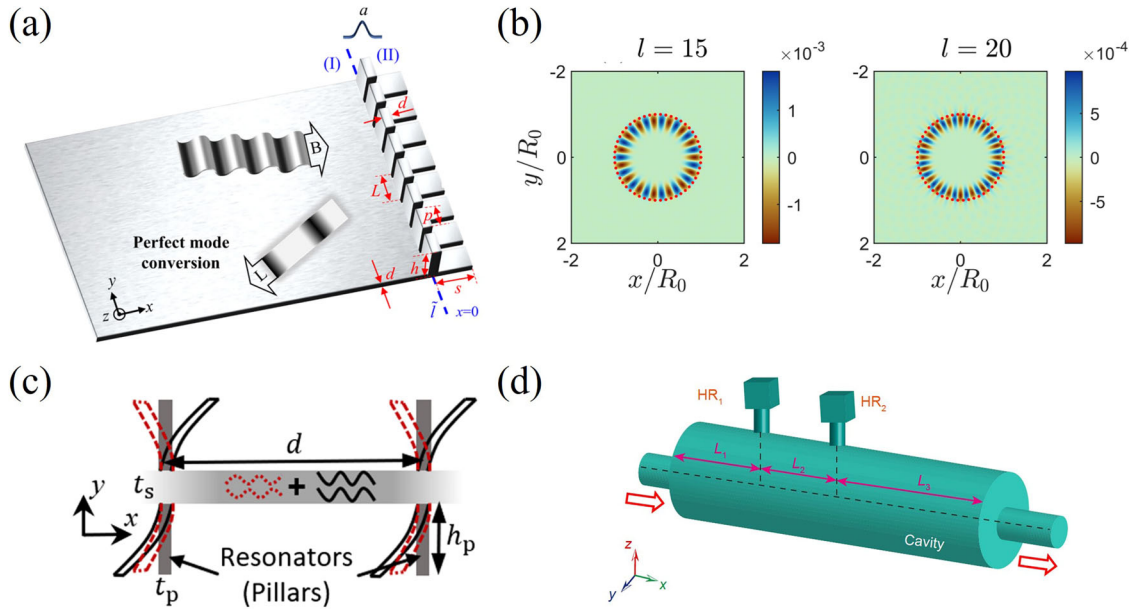

Fig. 3 | BICs in elastic and topological systems. a Elastic-wave trapped mode with perfect mode conversion between flexural and longitudinal waves. **b** Whispering gallery modes with different resonant index formed by clusters of highly symmetric scatterers. **c** Multibranch Lamb wave quasi-BICs realized by side-branch resonance pillars. **d** Topological BICs induced extreme asymmetric acoustic transmission by FP cavity side-branch Helmholtz resonators. **a** is adapted from ref. 51 with permission, Copyright 2021 Elsevier Ltd.; **b** is adapted from ref. 57 with permission, CC BY 4.0; **c** is adapted from ref. 60 with permission, Copyright 2024 American Physical Society; **d** is adapted from ref. 67 with permission, Copyright 2023 Science China Press.

Topological BICs

Another starting research direction attempts to link the robustness of BICs with topological physics, namely the so-called topological BICs. Several works confirming the relationship between BICs and topological properties have been carried out for electromagnetic waves[61–63]. The topic of BICs in the field of mechanical waves, which is our focus, has been gradually following up due to the excellent sources of experimental verification. Xiao et al. [64] found that the one-dimensional interface state composed of different topological phases can coexist with the extended state in the continuum, and this state can be regarded as a topological BICs. They experimentally confirmed this idea in a one-dimensional phononic crystal consisting of acoustic resonators. Chen et al. [65] identified one type of corner state in the two-dimensional system as BICs. They clearly showed from both the analysis of the tight-binding model and the numerical simulation of acoustic topological insulators that this type of corner state belongs to the continuum frequency range, which is supposed to radiate, but can still remain as a mode without leakage. Xia et al. [66] demonstrated the topological bound states by introducing the disclinations of lattices into the elastic phononic plate. Their work shows that the bound states captured by disclinations can avoid the influence of interfering factors, such as the finite size and defects of the plate while maintaining high-quality local effects. Zhang et al. [67] designed a structure with two Helmholtz resonators on the side branches of the FP cavity to realize topological BICs, as shown in Fig. 3d. One of them is located at the node of the standing wave field, forming a trivial BIC. The other provides an additional resonance to change the topological properties. By adjusting its position, the loss factor of the system can be controlled, which can cause two singular points carrying opposite topological charges to merge and form topological BICs. This merged EP has an extremely asymmetric property, that is, the energy incident from one direction is confined to the Helmholtz resonator at the node due to the formation of topological BICs, while that incident from the other is almost completely reflected. Pu et al. [68] theoretically proposed the bound hinge states in the continuum (BHICs) based on a parallelogram prism phononic crystal. Their research shows that the high-order topological insulator formed by this structure has two groups of triangular Weyl complexes. Each of them maintains a conventional hinge state connecting the Weyl points or extending to the boundary of the Brillouin zone. However, a hinge state that completely crosses the entire Brillouin zone appears in the bulk band between the two triangular Weyl complexes, which is the so-called BHICs. They observed the conventional hinge states and BHICs through simulations and airborne acoustic experiments. Recently, Guo et al. [69] proposed a synthetic way to realize the merged topological corner states in the continuum (MTCICs) and experimentally tested its evolution and performance in an acoustic cavity system. They constructed high-order topological insulators with corner states by introducing a physical parameter as the synthetic dimension to the two-dimensional generalized Aubry-André-Harper model. On this basis, they further proposed a double-layer structure by mirror-stacking two equal basic structures, and the two corner states are merged in the energy spectrum and real space by adjusting the interlayer coupling to form the MTCICs.

The intervention of topology will increase the consideration of robustness and defect resistance in the study of BICs, which will help develop mechanical devices suitable for environments that require high robustness. At the same time, some non-Hermitian characteristics, such as the concept of EPs, may bring innovations to the study of topological BICs.

BICs in Optomechanics

BICs have also been studied in the context of optomechanical devices, with promising results for ultra-sensitivity and information processing[70], even reaching the quantum regime (e.g. quantum transduction)[71–73]. Under a "macroscopic" view, it is already well known that in photonic crystals, cavities, and finite scatterers, optical modes can strongly interact with acoustic ones via radiation pressure forces[45,72,74]. Many excellent reviews about the origin of such interaction can be found in the literature, for instance in ref. 75. Review[75] summarizes the relevant optomechanical parameters for some implementations that are being currently used for excitation of BICs or QBICs.

As optomechanics mostly deals with two coupled fields, the reduction of both optical and mechanical (clamping) losses is crucial for incoming searches of BICs and high-Q resonance-based devices[44]. One way to achieve reduced losses consists of designing strategic band gaps around the modes of interest in the phase space. However, a smarter strategy to avoid leakage would seize the framework of BICs, which involves multi-parametric spaces, to sketch devices. A simple, appropriate combination of geometry and

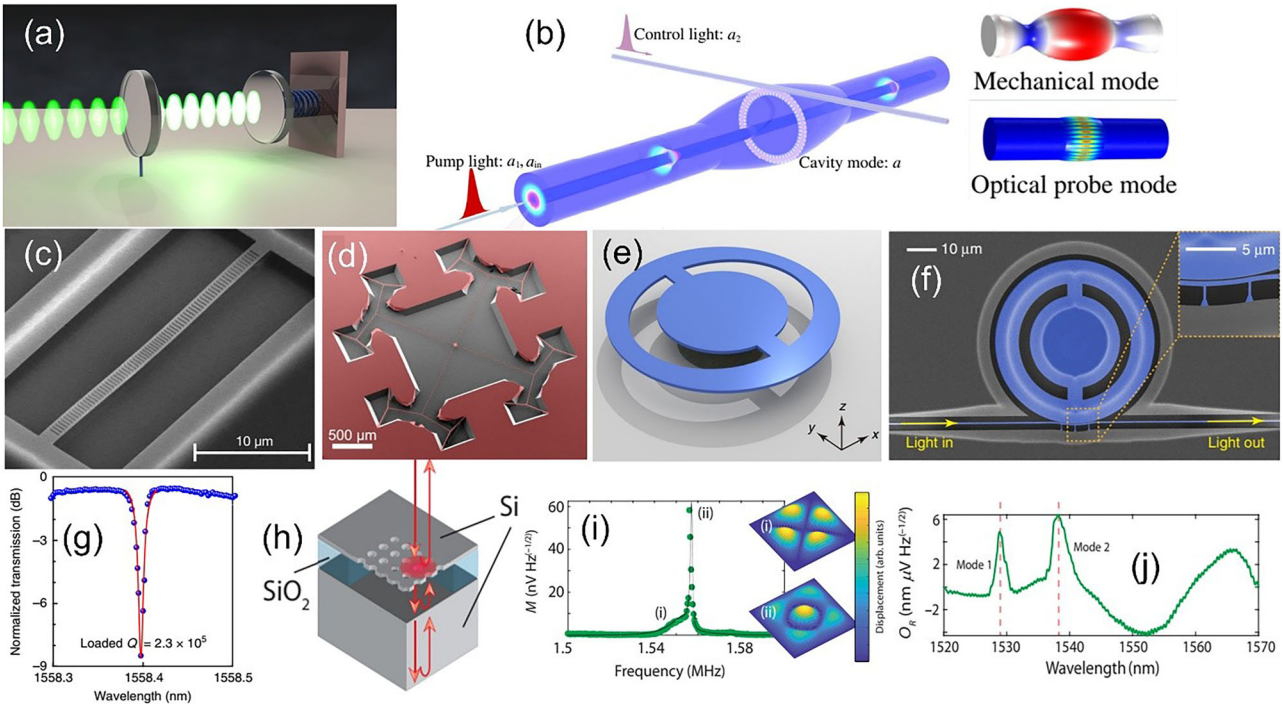

Fig. 4 | BICs in optomechanical systems. a Typical setup for optomechanics based on the Fabry-Pérot geometry. **b** fiber-based optomechanical system, which does not require phase matching or cavity enhancement of the pump beam. The inset on the right shows the modal shapes in such scheme. **c** Silicon nanobeam optomechanical crystal. **d** Trampoline membranes with partial soft-clamping, as an example of the improvement in fabrication techniques to obtain high-quality resonances. **e–g** Micromechanical resonator to measure mechanical BICs via optomechanical coupling; **e** geometry, **f** photograph of the configuration to show how light is coupled to the structure. The inset is a close-up showing the details in the coupling region of the resonator and bus waveguide. **g** Zoom of the optical transmission spectrum obtained, showing a resonance with Lorentzian-fitted (optical) Q factor that can be tracked to a later detection of a mechanical BIC. **h–j** A relatively simple, useful device to introduce optomechanical modulation spectroscopy (OMS), which can be used to characterize BICs through signal reconstruction using mechanically modulated signals. **h** The design consists of a Si metasurface suspended on a Si handle, combining metasurface modes and multiple reflections within the substrate and air layer; **i** shows the mechanical modes used to modulate the OMS. **j** After processing, the reconstructed signal clearly shows the location of two BICs, labeled Mode 1 and Mode 2 in the figure. **a** is adapted from ref. 84 with permission, CC BY 3.0; **b** is adapted from ref. 85 with permission, CC BY 4.0; **c** is adapted from ref. 82 with permission, Copyright 2009 Macmillan Publishers Limited; **d** is adapted from ref. 86 with permission, CC BY 4.0; **e–g** are adapted from ref. 46 with permission, CC BY 4.0; **h–j** are adapted from ref. 88 with permission, Copyright 2022 American Physical Society.

constitution can enable metamaterial microcavities to support QBICs at the desired parameter configuration. In ref. 76, a photonic crystal membrane suspended above a distributed Bragg reflector mirror was used as a building block of a metastructure. When implemented with GaAs and AlGaAs, optical quality factors of 5×10^5 were predicted[76,77]. Many crystals with multiple relevant properties, such as piezoelectric, acoustic, and optical have been reported as good candidates with high-quality optomechanical performance[78–81]. For instance, lithium niobate ($LiNbO_3$) is always a good candidate to fabricate high-quality photonic microcavities on a chip without the need for superior etching in the structures[78].

The heart of optomechanics lies upon the simultaneous confinement or overlapping of mechanical and optical modes, broadly facilitated by laser drives because lasers can greatly enhance electric fields and produce strong light-matter interactions[82,83]. In a standard Fabry-Pérot configuration, Fig. 4a, a laser-driven optical cavity is enclosed between two mirrors, one of them is fixed while the other can vibrate[84]. By this simple setup, the optical modes can be modulated by the mechanical, but to turn modes into BICs, more complex setups are in general required to reduce losses and avoid energy leakage. Yet, some setups are preferable because they present relatively minimal complexity, such as fiber-based systems. In particular, the scheme shown in Fig. 4b was reported for coherent wavelength conversion with extremely high Q factors for both fields[85]. Simply put, a pump beam propagating in the fiber core exerts an optical force in the transverse direction to excite the mechanical motion. The mechanical motion modulates a probe field traveling in the fiber cladding in the transverse plane to generate an optical field with a new wavelength. This type of fiber coupling not only simplifies the implementation of coherent wavelength conversion but also extends the tuning bandwidth from MHz-GHz to tens of THz, which enables a broad range of coherent-optics-based applications with high-Q modes. To get QBICs, a few novel designs rely on soft cladding or meticulous arrangement to isolate the active part of the system and so improve the quality of its resonances, see for instance Fig. 4b-d[82–86]. Moreover, a new era of intricate metamaterials, including the recent optomechanical crystals have launched the engineering of BICs to explore the photon-phonon interaction beyond the framework of suspended microcavities[87]. Specifically, ref. 45 reported symmetry-protected BICs in a simple slab-substrate structure made of anisotropic elastic materials. However, these anisotropic crystals must be carefully studied in the framework of symmetry group theory since the symmetry-protected BICs may appear due to symmetry's incompatibility. An appropriate theoretical scenario, which includes advanced group theory and multi-parametric space manipulation is still lacking.

Optomechanics can be also used inversely to detect or measure a BIC. A remarkable example of observation of BICs through an optomechanical device can be found in ref. 46. In that work, the authors reported the detection of a mechanical BIC in an optomechanical microresonator by means of the readout variations due to the optomechanical coupling in the structure, Fig. 4e-g. By carefully designing the individual resonator and checking the robustness in its fabrication, Fig. 4e-f, the microresonator was shown to sustain BICs that can be explained by the FW formalism. Slight perturbations of the geometry within this framework allowed for FW QBIC identification. In this way, simple measurements of the light coupled to the structure by a nearby waveguide were enough to identify the QBIC as a sharp decrease in the optical transmission, Fig. 4g, which has its counterpart in the mechanical BIC excited.

In another example, a novel technique called optomechanical modulation spectroscopy was implemented to characterize a BIC in a Si metasurface[88], Fig. 4(h). In ref. 88 this technique was successfully used to detect QBICs in the structure, which were confirmed by FEM simulations. Briefly, let us suppose that we have an optical feature of interest buried in a wide background signal. This feature could be a mode localized in a photonic structure, while the background could be coming from an underlying substrate. Moreover, let us suppose that the two contributions, the "main" signal and its background, have different optomechanical couplings. Actuating a proper mechanical mode operating in mild vacuum, the modulated signals can be evaluated (Fig. 4i) leading to a reconstructed signal (Fig. 4j), where the relative amplitude of the different features has been rescaled according to the ratio of their own optomechanical couplings, resulting in a strongly enhanced feature visibility of an elusive feature[88].

As for the near future, one of the most remarkable applications of BICs in optomechanics is the trapping and manipulation of light, nanoparticles or subwavelength-sized structures[89–91], since they promise to contribute to nanorobot medicine, sensing, energy harvesting, colloidal assembly, and analog computing, among others[92]. Ref. 93 theoretically demonstrated that a slightly perturbed all-dielectric structure harnessed QBICs to enable the trapping of nanoscale objects with low laser power and a negligible heating effect. The QBICs system provides very high electromagnetic-field enhancement that is an order of magnitude higher than that for conventional plasmonic systems, as well as high-quality-factor resonances comparable to photonic crystal cavities.

Summary and Outlook

We present an insight into the theoretical foundation and experimental progress of BICs in acoustic, elastic, topological, and optomechanical systems. Originally formulated in quantum mechanics, BICs have since expanded into the realms of classical waves, notably acoustics and elasticity, where they exhibit the remarkable ability to trap energy with theoretically infinite quality factors. This property arises from mechanisms such as symmetry mismatch and destructive interference, which cancels energy leakage in open systems.

Focusing on mechanical BICs, this perspective gives the basic mechanisms of different types of BICs and surveys experimental breakthroughs that have validated the existence of BICs in practical settings, from waveguides and resonant cavities to optomechanical systems. It emphasizes how BICs have led to innovations in various technologies, including emission-enhancement, sensors, sound absorbers, filters, and optomechanical resonators. By synthesizing the latest theoretical models and experimental observations, we believe that the future research directions in the field of mechanical BICs are as follows:

(1) At the theoretical level, it is necessary to consider the exploration of different types of BIC mechanisms in a wider range of physical systems. Possible research topics include the involvement of gain and loss in non-Hermitian systems and the deep connection between topological theory and BICs in terms of energy confinement. In addition, in the process of constructing elastic non-Hermitian systems, a common method is to use the electromechanical coupling effect of piezoelectric materials to create gains and losses. This may lead to research on the regulation mechanism of BICs by multi-physics coupling, and even the influence of introducing time variables.

2) At the experimental level, the fabrication and observation of BICs with higher Q-factors remain the main topic and may involve more frequency ranges. For example, with the development of micro-nano processing and laser detection technology, observations in the MHz and GHz ranges should be an important direction. Moreover, due to the lag of experimental research relative to theoretical studies, experimental verification will be accompanied by the development of BICs' mechanisms in a wider range of physical systems.

3) At the application level, we believe that the incoming emission-enhancement devices, sensors, sound absorbers, filters, polarization converters, modulators, and optomechanical resonators, may use BIC-based technology. In other words, more designs based on high Q-factor devices should be foreseeable. These may include highly sensitive sensors for environment change (temperature, pressure, etc.), highly efficient sound absorbers for sound wave isolation, ultra-narrowband filters for acoustic signal processing, ultra-low-loss optomechanical systems for advancements in quantum and cosmological physics, and so forth.

Data availability

No datasets were generated or analysed during the current study.

Received: 25 October 2024; Accepted: 12 April 2025;
Published online: 03 July 2025

References

1. von Neumann, J. & Wigner, E. P. Über merkwürdige diskrete eigenwerte. *Physikalische Zeitschrif* **30**, 465 (1929).
2. Stillinger, F. H. & Herrick, D. R. Bound states in the continuum. *Phys. Rev. A* **11**, 446 (1975).
3. Hsu, C. W., Zhen, B., Stone, A. D., Joannopoulos, J. D. & Soljačić, M. Bound states in the continuum. *Nat. Rev. Mater.* **1**, 1 (2016).
4. Sadreev, A. F. Interference traps waves in an open system: bound states in the continuum. *Rep. Prog. Phys.* **84**, 055901 (2021).
5. Joseph, S., Pandey, S., Sarkar, S. & Joseph, J. Bound states in the continuum in resonant nanostructures: an overview of engineered materials for tailored applications. *Nanophotonics* **10**, 4175 (2021).
6. Azzam, S. I. & Kildishev, A. V. Photonic Bound States in the Continuum: From Basics to Applications. *Adv. Opt. Mater.* **9**, 2001469 (2020).
7. Kang, M., Liu, T., Chan, C. T. & Xiao, M. Applications of bound states in the continuum in photonics. *Nat. Rev. Phys.* **5**, 659 (2023).
8. Huang, L. et al. Acoustic resonances in non-Hermitian open systems. *Nat. Rev. Phys.* **6**, 11 (2023).
9. Parker, R. Resonance effects in wake shedding from parallel plates: Some experimental observations. *J. Sound Vib.* **4**, 62 (1966).
10. Parker, R. Resonance effects in wake shedding from parallel plates: Calculation of resonant frequencies. *J. Sound Vib.* **5**, 330 (1967).
11. Plotnik, Y. et al. Experimental observation of optical bound states in the continuum. *Phys. Rev. Lett.* **107**, 183901 (2011).
12. Jia, B. et al. Bound States in the Continuum Protected by Reduced Symmetry of Three-Dimensional Open Acoustic Resonators. *Phys. Rev. Appl.* **19**, 054001 (2023).
13. Ordonez, G., Na, K. & Kim, S. Bound states in the continuum in quantum-dot pairs. *Phys. Rev. A* **73**, 022113 (2006).
14. Hein, S., Koch, W. & Nannen, L. Trapped modes and Fano resonances in two-dimensional acoustical duct–cavity systems. *J. Fluid Mech.* **692**, 257 (2012).
15. Lepetit, T. & Kanté, B. Controlling multipolar radiation with symmetries for electromagnetic bound states in the continuum. *Phys. Rev. B* **90**, 241103 (2014).
16. Huang, S. et al. Extreme Sound Confinement From Quasibound States in the Continuum. *Phys. Rev. Appl.* **14**, 021001 (2020).
17. Friedrich, H. & Wintgen, D. Interfering resonances and bound states in the continuum. *Phys. Rev. A* **32**, 3231 (1985).
18. Huang, L. et al. General Framework of Bound States in the Continuum in an Open Acoustic Resonator. *Phys. Rev. Appl.* **18**, 054021 (2022).
19. Liu, S. et al. Observation of acoustic Friedrich-Wintgen bound state in the continuum with bridging near-field coupling. *Phys. Rev. Appl.* **20**, 044075 (2023).
20. Hsu, C. W. et al. Bloch surface eigenstates within the radiation continuum. *Light Sci. Appl.* **2**, e84 (2013).
21. Hsu, C. W. et al. Observation of trapped light within the radiation continuum. *Nature* **499**, 188 (2013).
22. Kikkawa, R., Nishida, M. & Kadoya, Y. Polarization-based branch selection of bound states in the continuum in dielectric waveguide modes anti-crossed by a metal grating. *N. J. Phys.* **21**, 113020 (2019).

23. Callan, M., Linton, C. M. & Evans, D. V. Trapped modes in two-dimensional waveguides. *J. Fluid Mech.* **229**, 51 (2006).
24. Evans, D. V. & Linton, C. M. Trapped modes in open channels. *J. Fluid Mech.* **225**, 153 (2006).
25. Evans, D. V., Levitin, M. & Vassiliev, D. Existence theorems for trapped modes. *J. Fluid Mech.* **261**, 21 (2006).
26. Sugimoto, N. & Imahori, H. Localized mode of sound in a waveguide with Helmholtz resonators. *J. Fluid Mech.* **546**, 89 (2006).
27. Lyapina, A. A., Maksimov, D. N., Pilipchuk, A. S. & Sadreev, A. F. Bound states in the continuum in open acoustic resonators. *J. Fluid Mech.* **780**, 370 (2015).
28. Lyapina, A. A., Pilipchuk, A. S. & Sadreev, A. F. Trapped modes in a non-axisymmetric cylindrical waveguide. *J. Sound Vib.* **421**, 48 (2018).
29. Sadreev, A., Bulgakov, E., Pilipchuk, A., Miroshnichenko, A. & Huang, L. Degenerate bound states in the continuum in square and triangular open acoustic resonators. *Phys. Rev. B* **106**, 085404 (2022).
30. Zangeneh-Nejad, F. & Fleury, R. Topological Fano Resonances. *Phys. Rev. Lett.* **122**, 014301 (2019).
31. Huang, L. et al. Sound trapping in an open resonator. *Nat. Commun.* **12**, 4819 (2021).
32. Huang, L. et al. Topological Supercavity Resonances in the Finite System. *Adv. Sci.* **9**, 2200257 (2022).
33. Yin, Y. et al. Accidental bound states in the continuum in acoustic resonators with rotating obstacles. *Phys. Rev. B* **110**, 054201 (2024).
34. Wang, X., Fang, X., Mao, D., Jing, Y. & Li, Y. Extremely Asymmetrical Acoustic Metasurface Mirror at the Exceptional Point. *Phys. Rev. Lett.* **123**, 214302 (2019).
35. Zhu, X., Ramezani, H., Shi, C., Zhu, J. & Zhang, X. PT-Symmetric Acoustics. *Phys. Rev. X* **4**, 031042 (2014).
36. Koshelev, K., Lepeshov, S., Liu, M., Bogdanov, A. & Kivshar, Y. Asymmetric Metasurfaces with High-Q Resonances Governed by Bound States in the Continuum. *Phys. Rev. Lett.* **121**, 193903 (2018).
37. Zhou, Z., Jia, B., Wang, N., Wang, X. & Li, Y. Observation of Perfectly-Chiral Exceptional Point via Bound State in the Continuum. *Phys. Rev. Lett.* **130**, 116101 (2023).
38. Krasikova, M. et al. Acoustic bound states in the continuum in coupled Helmholtz resonators. *Phys. Rev. Appl.* **22**, 024045 (2024).
39. Kronowetter, F. et al. Realistic prediction and engineering of high-Q modes to implement stable Fano resonances in acoustic devices. *Nat. Commun.* **14**, 6847 (2023).
40. Martí-Sabaté, M., Li, J., Djafari-Rouhani, B., Cummer, S. A. & Torrent, D. Observation of two-dimensional acoustic bound states in the continuum. *Commun. Phys.* **7**, 122 (2024).
41. Huang, S. et al. Acoustic Purcell effect induced by quasibound state in the continuum. *Fundamental Res.* **4**, 57 (2024).
42. Jin, Y., Djafari-Rouhani, B. & Torrent, D. Gradient index phononic crystals and metamaterials. *Nanophotonics* **8**, 685 (2019).
43. Wang, W. et al. Robust Fano resonance in a topological mechanical beam. *Phys. Rev. B* **101**, 024101 (2020).
44. Chen, Y. et al. Mechanical bound state in the continuum for optomechanical microresonators. *N. J. Phys.* **18**, 063031 (2016).
45. Zhao, M. & Fang, K. Mechanical bound states in the continuum for macroscopic optomechanics. *Opt. Express* **27**, 10138 (2019).
46. Yu, Y., Xi, X. & Sun, X. Observation of mechanical bound states in the continuum in an optomechanical microresonator. *Light Sci. Appl.* **11**, 328 (2022).
47. Tsaturyan, Y. et al. Demonstration of suppressed phonon tunneling losses in phononic bandgap shielded membrane resonators for high-Q optomechanics. *Opt. Express* **22**, 6810 (2014).
48. Anetsberger, G., Rivière, R., Schliesser, A., Arcizet, O. & Kippenberg, T. J. Ultralow-dissipation optomechanical resonators on a chip. *Nat. Photonics* **2**, 627 (2008).
49. Cole, G. D., Wilson-Rae, I., Werbach, K., Vanner, M. R. & Aspelmeyer, M. Phonon-tunnelling dissipation in mechanical resonators. *Nat. Commun.* **2**, 231 (2011).
50. Cao, L. et al. Perfect absorption of flexural waves induced by bound state in the continuum. *Extrem. Mech. Lett.* **47**, 101364 (2021).
51. Cao, L. et al. Elastic bound state in the continuum with perfect mode conversion. *J. Mech. Phys. Solids* **154**, 104502 (2021).
52. Haq, O. & Shabanov, S. Bound States in the Continuum in Elasticity. *Wave Motion* **103**, 102718 (2021).
53. Deriy, I., Toftul, I., Petrov, M. & Bogdanov, A. Bound States in the Continuum in Compact Acoustic Resonators. *Phys. Rev. Lett.* **128**, 084301 (2022).
54. Rahman, A. & Pal, R. K. Bound modes in the continuum based phononic waveguides. *J. Appl. Phys.* **132**, 115109 (2022).
55. Rahman, A. & Pal, R. K. Elastic bound modes in the continuum in architected beams. *Phys. Rev. Appl.* **21**, 024002 (2024).
56. Jin, Y., Y. Pennec, Y. & Djafari-Rouhani, B. Acoustic analogue of electromagnetically induced transparency and Autler–Townes splitting in pillared metasurfaces. *J. Phys. D: Appl. Phys*. **51** (2018).
57. Martí-Sabaté, M., Djafari-Rouhani, B. & Torrent, D. Bound states in the continuum in circular clusters of scatterers. *Phys. Rev. Res.* **5**, 013131 (2023).
58. Lee, D. et al. Elastic bound states in the continuum by acoustoelastic interaction. *Extrem. Mech. Lett.* **61**, 101965 (2023).
59. Gao, N., Abraham-Ekeroth, R. M. & Torrent, D. Bound states in the continuum for antisymmetric lamb modes in composite plates made of isotropic materials. *Wave Motion* **129**, 103348 (2024).
60. An, S. et al. Multibranch Elastic Bound States in the Continuum. *Phys. Rev. Lett.* **132**, 187202 (2024).
61. Zhen, B., Hsu, C. W., Lu, L., Stone, A. D. & Soljacic, M. Topological nature of optical bound states in the continuum. *Phys. Rev. Lett.* **113**, 257401 (2014).
62. Bulgakov, E. N. & Maksimov, D. N. Topological Bound States in the Continuum in Arrays of Dielectric Spheres. *Phys. Rev. Lett.* **118**, 267401 (2017).
63. Doeleman, H. M., Monticone, F., den Hollander, W., Alù, A. & Koenderink, A. F. Experimental observation of a polarization vortex at an optical bound state in the continuum. *Nat. Photonics* **12**, 397 (2018).
64. Xiao, Y. X., Ma, G., Zhang, Z. Q. & Chan, C. T. Topological Subspace-Induced Bound State in the Continuum. *Phys. Rev. Lett.* **118**, 166803 (2017).
65. Chen, Z.-G., Xu, C., Al Jahdali, R., Mei, J. & Wu, Y. Corner states in a second-order acoustic topological insulator as bound states in the continuum. *Phys. Rev. B* **100**, 075120 (2019).
66. Xia, B., Jiang, Z., Tong, L., Zheng, S. & Man, X. Topological bound states in elastic phononic plates induced by disclinations. *Acta Mech. Sin.* **38**, 521459 (2022).
67. Zhang, H. et al. Topological bound state in the continuum induced unidirectional acoustic perfect absorption. *Sci. China Phys. Mech. Astron.* **66**, 284311 (2023).
68. Pu, Z. et al. Acoustic Higher-Order Weyl Semimetal with Bound Hinge States in the Continuum. *Phys. Rev. Lett.* **130**, 116103 (2023).
69. Guo, J., Gu, Z. & Zhu, J. Realization of Merged Topological Corner States in the Continuum in Acoustic Crystals. *Phys. Rev. Lett.* **133**, 236603 (2024).
70. Stannigel, K. et al. Optomechanical quantum information processing with photons and phonons. *Phys. Rev. Lett.* **109**, 013603 (2012).
71. Ren, H. et al. Two-dimensional optomechanical crystal cavity with high quantum cooperativity. *Nat. Commun.* **11**, 3373 (2020).
72. Rojas Hurtado, C. B., Dickmann, J., Feilong Bruns, F., Siefke, T. & Kroker, S. Bound states in the continuum for optomechanical light control with dielectric metasurfaces. *Opt. Express* **28**, 20106 (2020).
73. Meystre, P. A short walk through quantum optomechanics. *Ann. der Phys.* **525**, 215 (2012).
74. Valero, A. C. et al. Superscattering emerging from the physics of bound states in the continuum. *Nat. Commun.* **14**, 4689 (2023).
75. Aspelmeyer, M., Kippenberg, T. J. & Marquardt, F. Cavity optomechanics. *Rev. Mod. Phys.* **86**, 1391 (2014).

76. Péralle, C., Manjeshwar, S. K., Ciers, A., Wieczorek, W. & Tassin, P. Quasibound states in the continuum in photonic crystal based optomechanical microcavities. *Phys. Rev. B* **109**, 035407 (2024).
77. Tong, H., Liu, S. & Fang, K. Merging mechanical bound states in the continuum in high-aspect-ratio phononic crystal gratings. *Commun. Phys.* **7**, 197 (2024).
78. Yu, Z. & Sun, X. Acousto-optic modulation of photonic bound state in the continuum. *Light Sci. Appl.* **9**, 1 (2020).
79. Wang, Y. et al. A review of gallium phosphide nanophotonics towards omnipotent nonlinear devices. *Nanophotonics* **13**, 3207 (2024).
80. Yuan, J. et al. Enhancing Brillouin Scattering with Chalcogenide Metasurfaces of Optical Bound States in the Continuum and Mechanical Resonances. *Laser Photonics Rev.* **2024**, 2400763 (2024).
81. Yuan, J., Li, P., Zhang, X., Feng, T. & Li, Z. Chalcogenide metasurface heterostructures for enhancing optomechanical interaction. *Opt. Commun.* **563**, 130599 (2024).
82. Eichenfield, M., Chan, J., Camacho, R. M., Vahala, K. J. & Painter, O. Optomechanical crystals. *Nature* **462**, 78 (2009).
83. Xu, W., Iyer, A., Jin, L., Set, S. Y. & Renninger, W. H. Strong optomechanical interactions with long-lived fundamental acoustic waves. *Optica* **10**, 206 (2023).
84. Favero, I. & Marquardt, F. Focus on optomechanics. *N. J. Phys.* **16**, 085006 (2014).
85. Xi, X., Zou, C.-L., Dong, C.-H. & Sun, X. Highly tunable broadband coherent wavelength conversion with a fiber-based optomechanical system. *Adv. Photonics* **4**, 056003 (2022).
86. Bereyhi, M. J. et al. Hierarchical tensile structures with ultralow mechanical dissipation. *Nat. Commun.* **13**, 3097 (2022).
87. Liu, S., Tong, H. & Fang, K. Optomechanical crystal with bound states in the continuum. *Nat. Commun.* **13**, 3187 (2022).
88. Zanotto, S. et al. Optomechanical Modulation Spectroscopy of Bound States in the Continuum in a Dielectric Metasurface. *Phys. Rev. Appl.* **17**, 044033 (2022).
89. Cai, K., Zhu, Y., Ma, Y., Xiang, J. & Chen, L. Optical trapping of nanoparticles using all-dielectric quasi-bound states in the continuum. *Opt. Commun.* **569**, 130838 (2024).
90. Kostyukov, A. S., Gerasimov, V. S., Ershov, A. E., Bulgakov, E. N. & Sadreev, A. F. Size-selective optical trapping of nanoparticles with bound states in the continuum. *Opt. Lasers Eng.* **171**, 107797 (2023).
91. Huang, J. et al. Light trapping and manipulation of quasibound states in continuum Ge2Sb2Se4Te metasurfaces. *Phys. Rev. B* **106**, 045416 (2022).
92. Le, N. D. et al. Super Bound States in the Continuum on a Photonic Flatband: Concept, Experimental Realization, and Optical Trapping Demonstration. *Phys. Rev. Lett.* **132**, 173802 (2024).
93. Yang, S., Hong, C., Jiang, Y. & Ndukaife, J. C. Nanoparticle Trapping in a Quasi-BIC System. *ACS Photonics* **8**, 1961 (2021).

Acknowledgements

This publication is part of the project PID2021-124814NBC22, funded by MCIN/AEI/10.13039/501100011033/ "FEDER A way of making Europe". We thank Project No. CNS2023-145510 funded by MCIN/AEI/10.13039/501100011033, "European Union NextGenerationEU/PRTR". This work was supported by DYNAMO project (101046489), funded by the European Union. Views and opinions expressed are however those of the authors only and do not necessarily reflect those of the European Union or European Innovation Council. Neither the European Union nor the granting authority can be held responsible for them. This work is supported by the National Natural Science Foundation of China (12272267, 12025403, 12327807), the Young Elite Scientists Sponsorship Program by CAST (2021QNRC001), the Shanghai Science and Technology Committee (Grant No. 22JC1404100), Shanghai Gaofeng Project for University Academic Program Development. L.H. acknowledges support from the China Scholarship Council (Grant No. 202306260084).

Author contributions

L.H.: conceptualization, data curation, formal analysis, writing-original draft, writing-review and editing. S.S.: data curation, formal analysis, writing-original draft. R.A.: data curation, formal analysis, writing-original draft, writing-review and editing. Y.J.: conceptualization, funding acquisition, project administration, supervision, writing-review and editing. Y.X.: writing-review. D.T.: conceptualization, funding acquisition, project administration, supervision, writing-review and editing.

Competing interests

The authors declare no competing interests.

Additional information

Correspondence and requests for materials should be addressed to Yabin Jin or Dani Torrent.